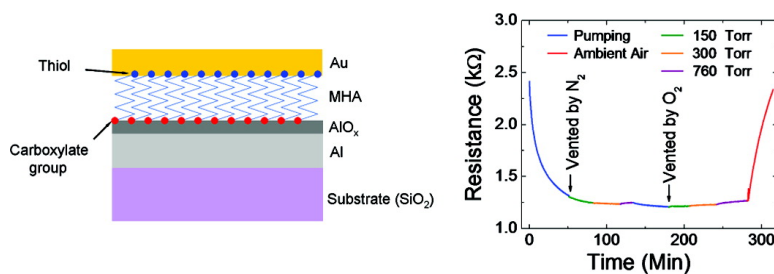


Origin of the Humidity Sensitivity of Al/AIO/MHA/Au Molecular Tunnel Junctions

Xiaohang Zhang, Stephen A. McGill, and Peng Xiong

J. Am. Chem. Soc., **2007**, 129 (46), 14470-14474 • DOI: 10.1021/ja0758988 • Publication Date (Web): 31 October 2007

Downloaded from <http://pubs.acs.org> on February 13, 2009



More About This Article

Additional resources and features associated with this article are available within the HTML version:

- Supporting Information
- Access to high resolution figures
- Links to articles and content related to this article
- Copyright permission to reproduce figures and/or text from this article

[View the Full Text HTML](#)



Origin of the Humidity Sensitivity of Al/AIO_x/MHA/Au Molecular Tunnel Junctions

Xiaohang Zhang, Stephen A. McGill,[†] and Peng Xiong*

Contribution from the Department of Physics and MARTECH, Florida State University, Tallahassee, Florida 32306

Received August 6, 2007; E-mail: xiong@martech.fsu.edu

Abstract: Electron tunneling spectroscopies have been performed on tunnel junctions incorporating mercaptohexadecanoic acid (MHA) between gold and surface-oxidized aluminum electrodes. Low-temperature superconducting conductance spectroscopy provides direct evidence for elastic tunneling across the junctions. At room temperature the electron transport of these junctions exhibits a high sensitivity to ambient humidity; the resistance of these devices drops by more than 50% when they are placed into a dry atmosphere or vacuum and recovers after they are returned to ambient air. By comparing these results to those obtained for similar junctions incorporating different molecular monolayers, it is determined that the interaction of water molecules with the AlO_x/carboxylate interface is the origin of the observed behavior. The tunneling spectra and the current–voltage characteristics indicate significant modifications of the barrier height of the AlO_x upon MHA binding and in the hydration of the molecular interface.

Introduction

As a fundamental building block of molecular electronics, molecular junctions in the form of various device structures¹ have been under intensive studies. The architectures include planar junctions,² nanopores,³ crossed nanowires,⁴ liquid metal drops,⁵ microsphere junctions,⁶ and single-molecule transistors,⁷ in addition to various scanning probes.⁸ While much progress has been made in the understanding of electron transport through molecular junctions, there continues to be a significant divergence of results from different device architectures and different research groups. The discrepancy poses a serious challenge in the effort to elucidate the intrinsic electronic properties of molecular junctions. The inconsistencies in the experimental results are often attributed to variations in the quality of the self-assembled monolayers (SAMs) and the nature of the molecule–electrode contacts.⁹ A factor that has received far

less attention is the environment. The electrical transport measurements are often carried out in ambient air or even in solvent. Penetration and adsorption of molecules such as water and oxygen into the SAM and/or the molecule–electrode interface are expected to strongly alter the electron transport. Recently, employing an open architecture of a microsphere junction, Long et al.⁶ observed a strong dependence of the charge transport on the water content in the environment, which they demonstrated as being due to the hydration of the Au–S contacts. The hydration effect raises intriguing questions about the mechanisms of electron transport at the molecular interface, and such observations exemplify the need for a systematic examination of the environmental effects on the electron transport in molecular junctions of different architecture and molecule–electrode interfaces in the effort to elucidate the intrinsic transport properties of molecular junctions and establish the efficacy of applications of molecular electronics in ambient environment.

Here we report on an investigation of electron tunneling spectroscopies, including superconducting conductance spectroscopy (SCS) and inelastic electron tunneling spectroscopy (IETS), on planar tunnel junctions incorporating a molecular monolayer of mercaptohexadecanoic acid [HS(CH₂)₁₅COOH, MHA] between a superconducting (Al) and a normal metal (Au) electrode. We chose MHA for its terminal groups (carboxylic for binding to AlO_x and thiol for binding to Au) and suitable carbon chain length (~2 nm). The SCS and current (*I*)–voltage (*V*) characteristics unambiguously establish direct elastic tunneling as the dominant transport mechanism in our junctions. At room temperature, we observe a pronounced increase in the junction resistance with environmental humidity. To the best of our knowledge, this is the first observation of such pronounced humidity dependence in molecular junctions of mac-

[†] Current address: National High Magnetic Field Laboratory, Florida State University, Tallahassee, FL 32310.

- (1) For a review, see: Joachim, C.; Ratner, M. A. *Proc. Natl. Acad. Sci. U.S.A.* **2005**, *102*, 8801.
- (2) Lodha, S.; Janes, D. B. *J. Appl. Phys.* **2006**, *100*, 024503.
- (3) Wang, W. Y.; Lee, T. H.; Reed, M. A. *Phys. Rev. B* **2003**, *68*, 035416.
- (4) Kushmerick, J. G.; Holt, D. B.; Yang, J. C.; Naciri, J.; Moore, M. H.; Shashidhar, R. *Phys. Rev. Lett.* **2002**, *89*, 086802.
- (5) Rampi, M. A.; Whitesides, G. M. *Chem. Phys.* **2002**, *281*, 373–391.
- (6) Long, D. P.; Lazorcik, J. L.; Mantooth, B. A.; Moore, M. H.; Ratner, M. A.; Troisi, A.; Yao, Y. X.; Cizek, J. W.; Tour, J. M.; Shashidhar, R. *Nat. Mater.* **2006**, *5*, 901.
- (7) (a) Park, J.; Pasupathy, A. N.; Goldsmith, J. I.; Chang, C.; Yaish, Y.; Petta, J. R.; Rinkoski, M.; Sethna, J. P.; Abruna, H. D.; McEuen, P. L.; Ralph, D. C. *Nature (London)* **2002**, *417*, 722. (b) Liang, W.; Shores, M. P.; Bockrath, M.; Long, J. R.; Park, H. *Nature (London)* **2002**, *417*, 725.
- (8) (a) Bumm, L. A.; Arnold, J. J.; Dunbar, T. D.; Allara, D. L.; Weiss, P. S. *J. Phys. Chem. B* **1999**, *103*, 8122–8127. (b) Cui, X. D.; Primak, A.; Zarate, X.; Tomfohr, J.; Sankey, O. F.; Moore, A. L.; Moore, T. A.; Gust, D.; Harris, G.; Lindsay, S. M. *Science* **2001**, *294*, 571.
- (9) (a) Salomon, A.; Cahen, D.; Lindsay, S.; Tomfohr, J.; Engelkes, V. B.; Frisbie, D. *Adv. Mater.* **2003**, *15*, 1881–1890. (b) Selzer, Y.; Cai, L. T.; Cabassi, M. A.; Yao, Y. X.; Tour, J. M.; Mayer, T. S.; Allara, D. L. *Nano Lett.* **2005**, *5*, 61–65.

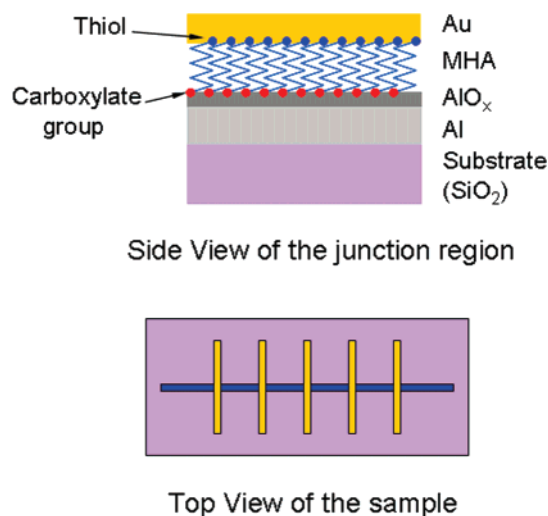


Figure 1. Schematic views of the junction structure (not to scale).

roscopic size or closed architecture. We demonstrate that the effect is directly linked to the interaction of water molecules with the carboxylate groups of the MHA SAM at the AIO_x surface. Analyses of the I - V produce compelling evidence for significant modifications of the tunnel barrier height of the AIO_x upon adsorption of the MHA SAM, and subsequently by the reaction of water molecules with the carboxylate group at the AIO_x surface. We attribute the barrier height changes to the alteration of the charge state in the AIO_x by the molecular binding and the hydration.

Experimental Methods

Junction Fabrication. The fabrication of tunnel junctions incorporating a layer of MHA between gold and surface-oxidized Al contacts is depicted in Figure 1. An Al stripe was thermally evaporated at 2.0×10^{-7} Torr through a shadow mask onto a Si substrate having a 100 nm thermally grown oxide. The thickness of the Al layer was around 50 Å (except in samples for IETS measurements, where the Al was about 700 Å thick). The ultrathin Al was necessary for the implementation of spin-polarized tunneling,¹⁰ the results of which will be reported elsewhere. After the evaporation, the sample was transferred to a pure oxygen environment in which surface oxidation was allowed to occur at room temperature for various intervals ranging from a few hours to 1 day. The sample was then placed into a 2 mM solution of MHA in ethanol, and a SAM was allowed to grow for 2–12 h. Fatty acids form SAMs on oxidized Al through the interaction between the oxide surface and the molecules' carboxylic group.¹¹ In the case of MHA, the thiol end is then exposed to make contact with the second metal layer. After rinsing with ethanol and drying the sample, five Au stripes were deposited by thermal evaporation at 2.0×10^{-7} Torr using a shadow mask. These stripes were oriented perpendicularly to the Al stripe and created five junctions. A low deposition rate (<0.1 Å/s) for the Au was used to minimize damage to and penetration through the MHA layer. The thickness of the Au stripes was 20 nm, and the finished junctions had an area of approximately 0.4×0.4 mm².

Measurements. Electron tunneling spectroscopy measurements were performed in a ³He cryostat (Oxford Heliox) with an 8-T superconducting magnet. The conductance spectrum was measured via first-harmonic phase-sensitive detection at a frequency of 17.3 Hz using a

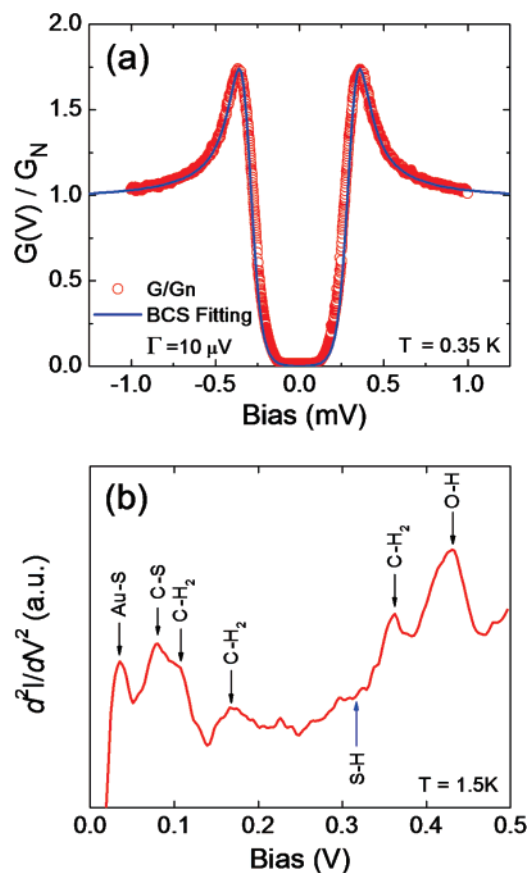


Figure 2. (a) Zero-field normalized conductance curve for an Al/AIO_x/MHA/Au junction and a BCS fitting with an inelastic scattering term of 10 μV. (b) IETS of an Al/AIO_x/MHA/Au junction. Relevant peaks are indicated by arrows.

PAR124A lock-in amplifier and a homemade direct current voltage sweeper. The IETS spectrum was measured on a different junction identically fabricated but with a much thicker Al electrode in order to avoid current crowding. An 8 mV alternating current modulation at 15.971 kHz was used, and the second harmonic signal was collected on an EG&G 7265 lock-in amplifier to obtain the IETS spectrum. Direct current I - V curves were obtained at room temperature by the standard four-terminal method with a Keithley 2400 sourcemeter.

The zero-bias resistance (R_J) of these junctions was measured at room temperature under various environmental conditions. R_J was monitored in the same probe used for low-temperature measurements as it was evacuated to vacuum and then back-filled with ambient air, dry N₂, or O₂. To further highlight and quantify the connection between R_J and the water vapor in the air, we also measured R_J as the relative humidity within a glovebox was controlled between 10% and 60% at 23 °C.

Results and Discussion

Tunneling Spectroscopy. Figure 2a shows a normalized conductance curve, dI/dV versus V , at 0.35 K and zero magnetic field for an Al/AIO_x/MHA/Au junction. The normalization was based on a bias sweep taken at a magnetic field slightly higher than the critical field of the Al film. This normalization procedure eliminates any energy-dependent normal state effects and tunnel barrier factors. Excellent fit to the Bardeen–Cooper–Schrieffer (BCS) superconducting density of states is obtained for the data in Figure 2a, with a negligible lifetime broadening¹² of 10 μeV. Both the subgap conductance and the lifetime

(10) Meservey, R.; Tedrow, P. M. *Phys. Rep.* **1994**, *238*, 173–243 (review section of *Phys. Lett.*).

(11) (a) Allara, D. L.; Nuzzo, R. G. *Langmuir* **1985**, *1*, 45–52. (b) Tao, Y. T. *J. Am. Chem. Soc.* **1993**, *115*, 4350–4358. (c) van den Brand, J.; Blajiev, O.; Beentjes, P. C. J.; Terryn, H.; de Wit, J. H. W. *Langmuir* **2004**, *20*, 6308.

(12) Dynes, R. C.; Narayanamurti, V.; Gamo, J. P. *Phys. Rev. Lett.* **1978**, *41*, 1509–1512.

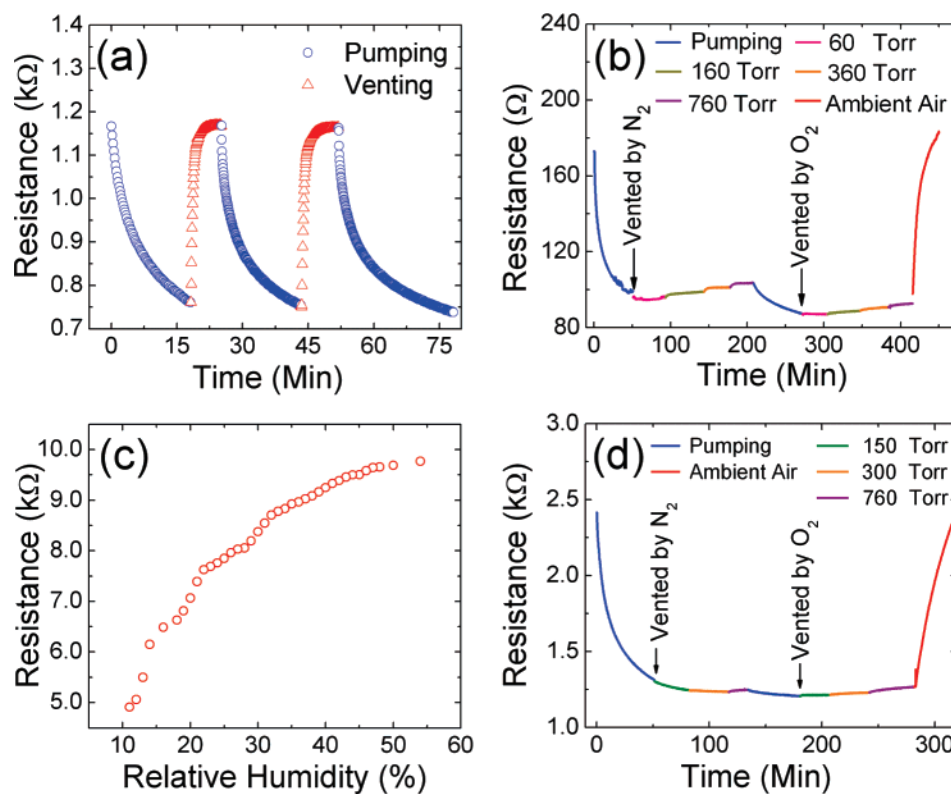


Figure 3. (a–c) Resistance variations of a junction with MHA with the environment. (a) The sample probe was evacuated and vented with ambient air repeatedly. (b) The sample probe was first pumped from ambient to vacuum and then back-filled with dry nitrogen to different pressure levels. The probe was pumped down to vacuum again and then back-filled with dry oxygen to different pressure levels. Eventually, the sample was returned into ambient. (c) The junction was set in a glovebox, the relative humidity of which was controlled between 10% and 60%. (d) Resistance variations of a junction with HDA under the same procedure as in (b). All measurements were performed at 296 K.

broadening are similar to those of an identically fabricated Al/AIO_x/Au junction without the MHA layer. Furthermore, the junction resistance exhibits a very weakly insulating temperature dependence, with $R_J(4\text{ K})/R_J(300\text{ K}) \approx 1.04$. These results are definitive signatures that the Al/AIO_x/MHA/Au junction is a high-quality tunnel junction. Figure 2b shows the IETS spectrum taken at 1.5 K. Because the high sheet resistance ($\sim 1\text{ k}\Omega$) of an ultrathin Al electrode in the normal state (either at high biases or temperatures above T_C) leads to current crowding, the IETS data were collected on a different junction identically fabricated but with a much thicker (700 Å) Al electrode to ensure accurate positioning of the inelastic peaks. Peaks corresponding to the bending and stretching vibration modes of C–S (80 meV), CH₂ (100, 160, and 360 meV), and OH (440 meV) can be clearly identified,^{13–15} along with the possible presence of C=O ($\sim 225\text{ meV}$ ¹⁶). Additionally, a pronounced peak is present at 33 meV. Although this peak is close to an acoustic phonon mode of Al (35 meV), other Al structures are absent in the spectrum.¹⁷ Both the position and the intensity of the peak are more consistent with $\nu(\text{Au–S})$.¹³ This observation, combined with the absence of the peak corresponding to S–H bonds ($\sim 320\text{ meV}$ ¹³), suggests that most of the thiol terminations of the MHA had reacted with the Au layer. The IETS results, coupled with

analysis of the I – V characteristics of the junction (shown later in Figure 4), demonstrate that direct elastic tunneling dominates the electron transport in these devices and that the tunneling does involve the MHA layer.

Water Sensitivity. The zero-bias resistance (R_J) of these junctions exhibited a large drop when placed into a vacuum from ambient air in preparation for the low-temperature transport measurements. As shown in Figure 3a, this effect was repeatable as the sample space of the probe was first evacuated and then back-filled with ambient air. A resistance change of $\sim 50\%$ was consistently observed in all measured junctions. In contrast, backfilling the evacuated space with *dry* N₂ and O₂ did not result in the recovery of R_J , as shown in Figure 3b. Exchanging ambient air with atmosphere dry N₂ resulted in a similar resistance change as a vacuum. The results of direct measurements of R_J as a function of the relative humidity in a glovebox at 23 °C are shown in Figure 3c. R_J approximately doubled as the relative humidity was increased from $\sim 10\%$ to 60%. These results demonstrate a direct correlation between the environment's water vapor content and changes in the junction resistance. The presence of the pronounced humidity sensitivity for such macroscopic-sized junctions with a closed architecture is somewhat surprising. The sheet resistance of the top Au electrode ($\sim 20\text{ nm}$ thick) is 30–40 Ω, indicating that the film is relatively uniform. Large-area AFM topography scan of the Au films on MHA showed absence of granularity. However, it is probable that grain boundaries exist which facilitate the diffusion of water molecules into and out of the MHA SAM.

(13) Wang, W. Y.; Lee, T. H.; Kretzschmar, I.; Reed, M. A. *Nano Lett.* **2004**, *4*, 643–646.

(14) Higo, M.; Kamata, S. *Anal. Sci.* **2002**, *18*, 227.

(15) Lambe, J.; Jaklevic, R. C. *Phys. Rev.* **1968**, *165*, 821.

(16) In IETS, the stretching mode of C=O in the carboxylate group is usually seen as a shifted and much broadened and diminished peak, compared to that in IR absorption. See ref 14.

(17) Petit, C.; Salace, G.; Vuillaume, D. *J. Appl. Phys.* **2004**, *96*, 5042.

In order to pinpoint the origin of the strong dependence of R_J on the relative humidity, we carried out a series of control experiments. First, Al/AIO_x/Au tunnel junctions were fabricated with an almost identical process which included immersion of the oxidized Al in ethanol (without MHA) for the same length of time. *These junctions without the MHA layer do not exhibit any resistance change with the relative humidity.* Next, we fabricated junctions having SAMs with different terminal groups in an effort to locate the interface that enables the sensitivity to water. We first replaced the thiol termination of MHA with a hydrophobic methyl group. In junctions incorporating a hexadecanoic acid [CH₃(CH₂)₁₄COOH, HDA] monolayer which preserves the COO⁻/AIO_x interface, a *quantitatively* similar (~50%) resistance change with humidity was observed, as shown in Figure 3d. In contrast, a significantly weaker effect was observed when the carboxylic group of MHA was replaced with a silane.¹⁸ Junctions incorporating octadecyltrichlorosilane [CH₃(CH₂)₁₇SiCl₃, OTS], which lacks both the carboxylic and thiol terminations, showed an average resistance change of ~5%, and one junction showed no change at all. Since the molecular backbones of each of these three molecules are fully saturated carbon chains, they are expected to have minimal interaction with water. Nevertheless, polar terminals can have a significant interaction with water. Moreover, because the trichlorosilanes of OTS are hydrolyzed during monolayer formation, it is possible that the small resistance changes observed in junctions with OTS also result from polar sites not passivated by the formation of the OTS layer. In the MHA junctions, both the Au–S interface and the COO⁻/AIO_x interface can interact with water and contribute to the resistance change. However, the *quantitative* similarities between the MHA junctions and HDA junctions suggest that water adsorption at the COO⁻/AIO_x interface is the primary cause of the resistance changes observed in our MHA junctions.

I–V Characteristic Analysis. To gain a basic understanding of the physical mechanism(s) behind the water sensitivity of the Al/AIO_x/MHA/Au junctions, we directly compare the *I–V* characteristics of junctions with and without an incorporated MHA layer in the theoretical framework developed by Simmons.¹⁹ Two junctions were fabricated simultaneously, differing only in that one contains MHA while the other does not. The surface-oxidized Al stripe not to be coated with MHA was stored in ethanol, while the other stripe was stored in an ethanol solution containing a 2 mM concentration of MHA. Figure 4 shows the *I–V* characteristics of the junction without MHA and the junction with MHA in vacuum and in ambient air. In the Simmons model, the tunneling current density is given by

$$J = J_0 \{ \Phi \exp(-A\Phi^{1/2}) - (\Phi + eV) \exp[-A(\Phi + eV)^{1/2}] \} \quad (1)$$

in which $J_0 = e/2\pi\hbar(\beta s)^2$, Φ is the average barrier height, $A = 4\pi\beta s(2m)^{1/2}/\hbar$, e is the electron charge, V is the bias voltage, s is the tunneling length, m is the electron mass, and β is a correction factor taken as unity in the model. The use of β less than unity was found necessary previously to produce good fits to *I–V* of some alkanethiol junctions,³ and it was attributed to effects of a non-rectangular barrier and effective electron mass. In our case, although the structure of the AIO_x/MHA barrier is

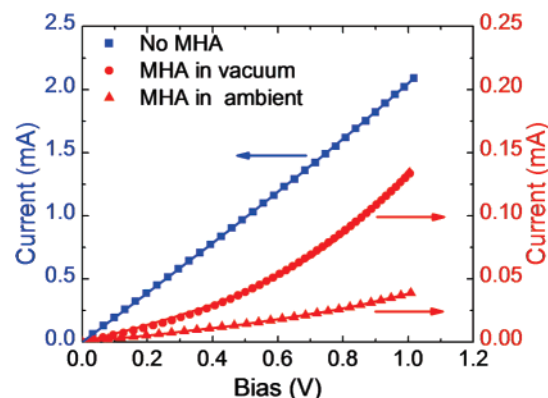


Figure 4. *I–V* data for a junction with MHA in vacuum and in ambient air, and a junction without MHA. Lines represent Simmons model fits as described in the text.

clearly asymmetric, due to the symmetric *I–V* we model the junction as having a single rectangular barrier²⁰ and analyze the *I–V* according to eq 1 with $\beta = 1$. Recently, a similarly asymmetric composite barrier of AIO_x and the organic semiconductor Alq₃ was found to result in little asymmetry in the tunneling spectra.²¹

The results of fitting the data with the smallest root-mean-square errors (RMSE) for these junctions are shown in Figure 4. The fits shown were obtained by using a convenient form of eq 1, obtained by replacing Φ with $(\Phi - eV/2)$ for an intermediate bias regime where $V < \Phi/e$. The best fit of the *I–V* curve for the Al/AIO_x/Au junction without MHA yields an average barrier height, $\Phi = 10.0$ eV, and tunneling length, $s = 7.1$ Å. The barrier height is surprisingly large (much greater than the band gap of bulk Al₂O₃). However, the results are in excellent agreement with values obtained from similar Al/AIO_x/Au junctions with naturally oxidized AIO_x barriers in a prior work,²² in which the large barrier height was attributed to uncompensated cations in the AIO_x. The incorporation of MHA, as measured in vacuum, leads to a large reduction in the average barrier height to 2.8 eV, while the tunneling distance increases to about 14.6 Å. Upon exposure of the junction to ambient air, the current decreases significantly at all biases, and R_J approximately doubles. The fitting of the *I–V* in air to eq 1 yields $\Phi = 4.1$ eV and $s = 12.7$ Å, indicating that hydration leads to a marked increase in the barrier height. As mentioned above, strictly, the application of the Simmons model requires the satisfaction of a set of stringent conditions.²⁰ However, *I–V* analyses of this type have been used effectively to deduce the barrier heights and widths in a wide variety of tunnel junctions. In our case, the fittings are all of high quality; more importantly, the uncertainties in the best fitting parameters are much smaller than the magnitudes of their variation with junction structure and environmental conditions. Specifically, a significant degradation in fitting quality (twice the RMSE of the best fits) results in the following changes in the barrier height and width: 1.5 eV and 0.5 Å, 0.4 eV and 1.0 Å, 0.3 eV and 0.4 Å, for the junction without MHA, the MHA junction in vacuum, and the MHA junction in ambient air, respectively. Therefore,

(20) Brinkman, W. F.; Dynes, R. C.; Rowell, J. M. *J. Appl. Phys.* **1970**, *41*, 1915.

(21) Santos, T. S.; Lee, J. S.; Migdal, P.; Lekshmi, I. C.; Satpati, B.; Moodera, J. S. *Phys. Rev. Lett.* **2007**, *98*, 016601.

(22) Gloos, K.; Koppinen, P. J.; Pekola, J. P. *J. Phys.: Condens. Matter* **2003**, *15*, 1733.

(18) Kessel, C. R.; Granick, S. *Langmuir* **1991**, *7*, 532–538.

(19) Simmons, J. G. *J. Appl. Phys.* **1963**, *34*, 1793.

the qualitative trend of the inferred variations of the barrier height and width with junction structure and humidity is unambiguous.

The correlation between the fitting results and the barrier structures provides important clues to the mechanism of electron transport through the molecular interface as well as its sensitivity to ambient humidity. First, the incorporation of MHA into the Al/AIO_x/Au junction results in an increase in tunneling distance and a substantial reduction in the average barrier height. This observation contradicts a simplistic model of a composite barrier with separate AIO_x and MHA layers. Attempts to fit the $I-V$ in this model invariably led to a negative barrier height for MHA ($\beta = 1$) or $\beta \ll 1$, which are clearly unphysical. Instead, our results point to a strong modification of the AIO_x barrier by the MHA SAM. The significant reduction of the AIO_x barrier height upon MHA binding can be understood as a result of the modification of the charge states in the AIO_x by MHA. In Al/AIO_x/Au junctions with naturally oxidized AIO_x barriers, Gloos et al.²² observed a pronounced dependence of the AIO_x barrier height on its thickness which they attributed to the variation of excess charges inside the barrier. Particularly, the unusually large (> 10 eV) barrier height in ultrathin AIO_x was believed to result from excess cations (unbound Al ions) in the barrier. Within this scenario, the binding of the carboxylate group of the MHA to the thin AIO_x neutralizes some of the excess cations and naturally leads to the reduction in the barrier height. The modification of interfacial dipoles²³ by the MHA binding could also contribute to the change in barrier height, although we expect the alteration of the charge state to be the dominant factor.

The observed effect of ambient humidity on the molecular junction transport can be naturally understood along the same line. Upon hydration of the junction, a large decline in tunneling current and an increase of junction resistance were observed. A naive explanation for the observation is a swelling of the junction width by water adsorption, which naturally results in an increase of the tunneling length. However, fitting of the $I-V$ taken in ambient air yields a *decrease* of the junction width to 12.7 Å and an *increase* of the average barrier height to 4.1 eV ($\beta = 1$) compared to the values in vacuum. The result suggests a different scenario for the effects of water adsorption on the molecular junction transport. The observation is consistent with a weakening of the coupling of the carboxylate group with the AIO_x by H₂O. In a recent report of hydration effect on microsphere thiol-Au junctions,⁶ IETS was used to probe the S-Au bonding before and after exposure to H₂O; the experiment established that most of the S-Au bonds were converted to S-H by H₂O. In our case, due to the rapid dehydration of the junctions in vacuum, we were unable to obtain similar IETS data on hydrated junctions at low temperature. However, it is reasonable to assume that a similar weakening of the COO⁻ bond to AIO_x occurs through water adsorption and formation

(23) Hamadani, B. H.; Corley, D. A.; Ciszek, J. W.; Tour, J. M.; Natelson, D. *Nano Lett.* **2006**, *6*, 1303.

of COOH because of the similar oxidizing properties of sulfur and oxygen. As a result, the hydration of the junction leads to an increase of the number of unbound cations in the AIO_x and, consequently, an increase in the barrier height.

An important issue in the study of molecular junctions is the reproducibility of the results. We have fabricated over 10 Al/AIO_x/MHA/Au junctions. Although the junction resistance varied from sample to sample, we always observed BCS-like conductance spectrum at low temperatures and similar humidity sensitivity at room temperature. Simmons $I-V$ fittings were carried out on several of these junctions, and the resulting fitting parameters always exhibited qualitatively similar trends in the variations of the barrier height and width with environmental humidity.

Finally, for junctions of such macroscopic size, there are almost certainly defects in the MHA SAM. The question is whether the electron transport across the junction is dominated by shorts through the defects, i.e., tunneling through the oxide layer only. There are several observations that are inconsistent with this scenario. First, the $I-V$ curves for the junctions with and without MHA clearly do not scale onto each other, as would be expected in the case where the current is carried by shorts through the organic layer. Furthermore, junctions incorporating MHA show high sensitivity to ambient humidity while Al/AIO_x/Au junctions are absent of any such effect. Therefore, the electron transport in Al/AIO_x/MHA/Au junctions likely incorporates significant contribution from tunneling through the MHA.

Conclusion

We have fabricated high-quality tunnel junctions that incorporate a superconducting electrode and an organic SAM layer in the barrier. The electron transport in the molecular tunnel junctions with the MHA SAM was shown to be sensitively dependent on the presence of water vapor, and the carboxylate-aluminum oxide interface was determined to be the location of the effect. A comparison of the results from the analysis of the $I-V$ curves of the junctions with and without the MHA layer indicates that the binding of MHA to AIO_x significantly lowers its barrier height; a similar comparison of the $I-V$ of the junction with MHA under vacuum and ambient conditions indicates an increase of the tunneling barrier height upon hydration of the MHA/AIO_x interface, which is responsible for the pronounced reduction in tunneling current and increase in junction resistance. We attribute the changes of the barrier height to the modification of the charge state in the AIO_x by the molecular binding and the hydration. Our results demonstrate that environmental effects could significantly impact the electron transport even in molecular junctions of macroscopic dimensions and closed architecture.

Acknowledgment. This work was supported by NSF NIRT grant ECS-0210332 and an FSURF PEG.

JA0758988